J. Fluid Mech. (2008), *vol.* 606, *pp.* 417–432.
doi:10.1017/S0022112008001997 Printed in the United Kingdom

Streamline topology near non-simple degenerate critical points in two-dimensional flow with symmetry about an axis

A. DELİCEOĞLU AND F. GÜRCAN†
Department of Mathematics, Erciyes University, Kayseri, Turkey 38039

(Received 29 April 2007 and in revised form 9 April 2008)

The local flow patterns and their bifurcations associated with non-simple degenerate critical points appearing away from boundaries are investigated under the symmetric condition about a straight line in two-dimensional incompressible flow. These flow patterns are determined via a bifurcation analysis of polynomial expansions of the streamfunction in the proximity of the degenerate critical points. The normal form transformation is used in order to construct a simple streamfunction family, which classifies all possible local streamline topologies for given order of degeneracy (degeneracies of order three and four are considered). The relation between local and global flow patterns is exemplified by a cavity flow.

1. Introduction

There are very few known exact solutions of the Navier–Stokes equations of viscous fluid dynamics. Milne-Thomson (1957, 1968) obtained the first general solution of the Navier–Stokes equations. Since this solution is given in the implicit form and is not resolved completely, it did not receive much attention. Without having to find a complete solution of the Navier–Stokes equations, global streamline patterns can often be deduced from an analysis of the flow behaviour local to stagnation points. This idea has long been familiar in dynamical systems theory and from the topological viewpoint, flows have been the subject of a considerable amount of work in fluid mechanics (e.g. see Legendre 1956; Tobak & Peake 1982; Dallmann 1983; Bakker 1991; Dallmann & Gebing 1994; Brøns & Hartnack 1999; Hartnack 1999*a*; Brøns, Voigt & Sørensen 2001; Brøns 2007).

In the present work we study streamline topology of two-dimensional incompressible flow near critical points (i.e. instantaneous stagnation points) which are degenerate in the sense that the Jacobian of the linearization of the corresponding Hamiltonian dynamical system about such a critical point vanishes identically. This paper is a follow-up of previous studies (Brøns & Hartnack 1999; Hartnack 1999*b*) investigating streamline topology near critical points (simple $\boldsymbol{J} \neq 0$ or non-simple $\boldsymbol{J} = 0$) of two-dimensional flow both near and away from boundaries. The first case concerning simple degenerate critical points (i.e. singular yet non-zero Jacobian matrix) is examined by Brøns & Hartnack (1999); we consider non-simple degenerate critical points (i.e. vanishing Jacobian) and thus it is complementary to Gürcan & Deliceoğlu (2005).

In the case of a zero Jacobian matrix, the local flow patterns can be determined by considering higher-order terms of the system. Since the resulting number of

† Author to whom correspondence should be addressed: gurcan@erciyes.edu.tr

free parameters is large, the bifurcation analysis about a non-simple degenerate critical point is complicated. However, using the idea of Brøns & Hartnack (1999) of normal form transformations, one can obtain a much simplified system of differential equations for streamlines encapsulating all the features of the original system. This approach has been used to analyse a variety of specific steady flows, for example the flow in a driven cavity (Gürcan & Deliceoğlu 2005), slip flows (Tophøj, Møller & Brøns, 2006), a flow close to fixed (possibly curved) walls (Hartnack, 1999*b*), a flow close to an interface (Brøns 1994), an axisymmetric flow (Bisgaard, Brøns & Sørensen 2006), and vortex breakdown (Brøns, Voight & Sørensen 1999; Brøns & Bisgaard 2006).

When the corresponding Hamiltonian dynamical system can be put into the simplest form by normal form transformations, we can obtain all possible degenerate streamline patterns for given degeneracies. The unfolding of the degenerate patterns, which means a family of streamfunctions containing a particular degenerate flow, will be obtained up to codimension three. These degenerate patterns are classified by their codimension, which is the number of their unfolding parameters. For codimension two, corresponding to the third-order normal form of the streamfunction, we obtain a flow pattern having critical points on a triangle connected with a single heteroclinic connection. In the case of flows near a wall, such a pattern has been predicted by the theoretical work of Bakker (1991) and Hartnack (1999*b*), in which two of the critical points lie on the wall, with the wall itself forming one side of the triangle. Brøns (1994) observed a similar structure away from boundaries for the flow close to a given streamline. Also Hartnack (1999*a*) found this for general unfolding of a double degeneracy found without any symmetry assumptions for codimension two. The same structure can be realized away from the boundaries in Stokes flow within a double-lid-driven rectangular cavity having two physical parameters.

Many authors have studied this type of cavity flow (for example, see Gürcan 1997; Chien, Rising & Ottino 1986; Meleshko 1996; Shankar & Deshpande 2000). Recently, Gürcan (2003) investigated streamline topologies near a non-simple degenerate critical point away from boundaries for small (height to width) aspect ratio A using both analytic solutions and methods from nonlinear dynamical systems. Gürcan *et al.* (2003) considered the analytic solution for the streamfunction, ψ, as a truncated series of Papkovich–Faddle eigenfunctions expanded about any stagnation point to reveal changes in the local flow structure as A and S are varied, where S is the speed ratio of the lid velocities. A particular region of S, A parameter space, $A \in (0, 3.2)$ and $S \in [-1, 0)$, was considered to construct a control-space diagram exhibiting several critical curves representing flow bifurcations at degenerate critical points. We use a similar idea to construct a bifurcation diagram for the triangle bifurcation. This is discussed later as an application of the theoretical framework developed in the next section.

In the present study, we also consider codimension three, corresponding to the fourth-order normal form of the streamfunction, to investigate streamline topologies. New flow patterns in Stokes flows are found and illustrated in a bifurcation diagram which is constructed using the parameterization method. We show that the Navier–Stokes equations do impose constraints on the local topology of steady flows.

2. Streamline topologies near non-simple degenerate critical points

Consider an incompressible two-dimensional flow far from any boundaries in x, y-coordinates with corresponding velocity components (u, v). A streamfunction ψ

exists such that the streamlines are found from

$$\dot{x} = u = \frac{\partial \psi}{\partial y}\ , \quad \dot{y} = v = -\frac{\partial \psi}{\partial x}\ . \tag{1}$$

To obtain local information about the flow close to a given point that is taken as the origin, ψ is expanded in a Taylor series

$$\psi = \sum_{i,j=0}^{\infty} a_{i,j} x^i y^j. \tag{2}$$

Let ψ be a given streamfunction satisfying

$$\psi(x, y) = \psi(-x, y), \tag{3}$$

which implies that the streamlines are mirror symmetric about the y-axis. Then we have

$$\psi = \sum_{i,j=0}^{\infty} a_{2i,j} x^{2i} y^j. \tag{4}$$

Hartnack (1999*a*) derived the normal form for $N = 3$ (codimension two) in the general case with no symmetries, and analysed it in detail.

The coefficients of the streamfunction can be explained in terms of the physical aspects, namely, derivatives of viscous stress tensor, pressure and derivatives of pressure. The viscous stress tensor is

$$\tau_{i,j} = \mu\left(\frac{\partial u_i}{\partial x_j} + \frac{\partial u_j}{\partial x_i}\right) \tag{5}$$

where μ is the dynamic viscosity of the fluid. Applying (5) and the Navier–Stokes equations one can verify the following relations:

$$\left.\begin{array}{lll} u(0,0) = a_{0,1}, & \tau_{xy} = 2\mu(a_{0,2} - a_{2,0}), & \dfrac{\partial \tau_{xx}}{\partial x} = 2\mu a_{2,1} \\ \dfrac{\partial p}{\partial x} = \rho\mu(2a_{2,1} + 6a_{0,3}), & \dfrac{\partial p}{\partial y} = \rho a_{0,1} a_{2,0} & \end{array}\right\} \tag{6}$$

where μ, ρ, p are the viscosity, density and pressure, respectively. The relations (5) and (6) between the expansion coefficients of ψ and the stress are also well-known, e.g. Brøns (1994) or Hartnack (1999*a*).

By using (4), equation (1) leads to a dynamical system,

$$\left.\begin{array}{l} \dot{x} = a_{0,1} + 2a_{0,2}y + a_{2,1}x^2 + 3a_{0,3}y^2 + 4a_{0,4}y^3 + 2a_{2,2}x^2 y + \cdots\ , \\ \dot{y} = -2a_{2,0}x - 2a_{2,1}xy - 2a_{2,2}xy^2 - 4a_{4,0}x^3 - \cdots\ . \end{array}\right\} \tag{7}$$

If $a_{0,1} = 0$ in (7), that is, the component of the vector u vanishes in the degeneracy, the origin becomes a critical point. Linearizing the system at that point produces the Jacobian matrix

$$\boldsymbol{J} = \begin{pmatrix} 0 & 2a_{0,2} \\ -2a_{2,0} & 0 \end{pmatrix}. \tag{8}$$

If $a_{2,0} = 0$ (i.e $\det(\boldsymbol{J}) = 0$) the critical point becomes a simple degenerate point and higher-order terms of ψ are needed to determine the local streamline patterns. This case was investigated by Brøns & Hartnack (1999) who considered the degenerate streamfunction ($\psi = a_{0,2}y^2 + \tilde{a}_{2N}x^{2N}$ where $N \geqslant 2$ and $\tilde{a}_{2N} \neq 0$). In their work all critical points lie on the x-axis (one on each side of the y-axis) and the shear stress

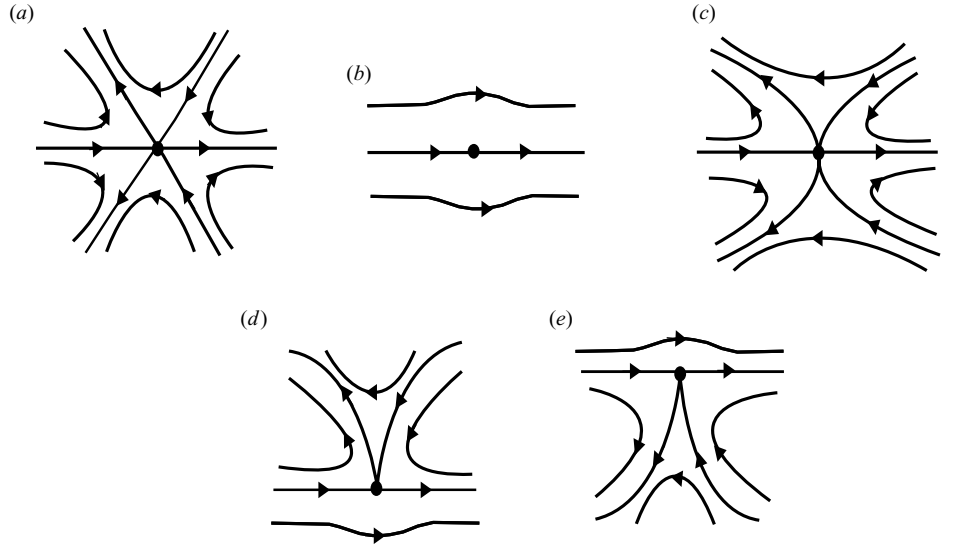

FIGURE 1. Non-simple degenerate critical points ($\tau_{xx} = \tau_{xy} = 0,\ \partial p/\partial x \neq 0$). (*a*) $a_{0,3}/a_{2,1} < 0$; (*b*) $a_{0,3}/a_{2,1} > 0$; (*c*) $\tilde{a}_{0,N}/a_{2,1} < 0$, $N > 4$ is odd; (*d*); (*e*) N is even and $N > 3$.

$a_{0,2} = \tau_{xy}/2\mu \neq 0$. This is a very restricted case for streamline patterns since the critical points coincide with the vertices of a triangle; two located on the x-axis (spanning the base of the triangle) and one located on the y-axis (the 'off-axis' point) cannot appear in unfolding with simple linear degeneracy. Here, we extend the study of Brøns & Hartnack (1999) to a zero Jacobian matrix, which gives a non-simple degeneracy, by assuming an extra condition, $a_{0,2} = 0$. This condition indicates that a degenerate flow pattern is formed where the component of the vector u and the shear stress τ_{xy} vanish simultaneously. In addition, it increases the degeneracy with codimension three since the streamfunction has the third-order terms $a_{2,1}$ and $a_{0,3}$ which gives the opportunity to take the critical points to coincide with the vertices of a triangle, and hence more possible flow patterns near the non-simple degenerate point may be obtained. From the assumptions of non-simple degeneracy and the mirror symmetry condition, one obtains the generic streamfunction corresponding to the type of critical points under investigation

$$\begin{aligned}\psi = {} & a_{2,1}x^2y + a_{0,3}y^3 + a_{0,4}y^4 + a_{2,2}x^2y^2 + a_{4,0}x^4 + a_{0,5}y^5 \\ & + a_{2,3}x^2y^3 + a_{4,1}x^4y + O((x, y)^6).\end{aligned} \tag{9}$$

Two fundamental cases can be considered in equation (9): (i) $a_{0,3} \neq 0$ and (ii) $a_{0,3} = 0$. In the first case ($a_{0,3} \neq 0$), we have only two terms of order three. By dropping the higher-order terms, the degenerate flow patterns can be found for $\psi = 0$, that is

$$y = 0, \qquad x = \pm\sqrt{-\frac{a_{0,3}}{a_{2,1}}}\,y. \tag{10}$$

For $a_{0,3}/a_{2,1} < 0$, there are six separatrices from a single saddle point, and this case is denoted a topological saddle, see figure 1(*a*). When $a_{0,3}/a_{2,1} > 0$, there are no separatrices except $y = 0$, figure 1(*b*).

In case (ii) with $a_{0,3}$ vanishing identically (i.e. the critical point coincides with the origin), the streamfunction (9) becomes

$$\psi = a_{2,1}x^2y + a_{0,4}y^4 + a_{2,2}x^2y^2 + a_{4,0}x^4 + a_{0,5}y^5 + a_{2,3}x^2y^3 + a_{4,1}x^4y + O((x, y)^6), \tag{11}$$

where the critical point is nonlinear degenerate to order four and higher-order terms in the expansion of ψ must be computed. To eliminate higher-order terms in (11) and for easy determination of the codimension, we use the idea of the normal form theory of Brøns & Hartnack (1999) by choosing a different generating function preserving the condition (3). An application of the theory to (11) (the detailed computations can be found in Brøns & Hartnack 1999 and Gürcan & Deliceoglu 2005), gives the normal form of (11) as indicated in the following theorem.

THEOREM 2.1. *Let $a_{0,3}$, $a_{0,4}$, $\widetilde{a}_{0,5}, \ldots, \widetilde{a}_{0,N-1}$ become zero. Assume the non-degeneracy conditions $a_{2,1} \neq 0$ and $\widetilde{a}_{0,N} \neq 0$ hold, then the normal form of order $N \geqslant 4$ for the streamfunction (11) is*

$$\psi = a_{2,1}x^2y + \widetilde{a}_{0,N}y^N \tag{12}$$

where $\widetilde{a}_{0,j}$, $j = 5, \ldots, N$ are transformed small parameters.

From the theorem, the local flow topology in the neighbourhood of the degenerate critical point can easily be obtained. Possible separatrices (dividing streamlines) of the critical point are given by $\psi = 0$, that is

$$y = 0, \qquad x = \pm\sqrt{-\frac{\widetilde{a}_{0,N}}{a_{2,1}}y^{N-1}}. \tag{13}$$

First we consider odd N. For $N \geqslant 5$ and $\widetilde{a}_{0,N}/a_{2,1} > 0$, the flow pattern is the same as in figure 1(*b*); for the pattern corresponding to $\widetilde{a}_{0,N}/a_{2,1} < 0$, see figure 1(*c*). If N is even and $N \geqslant 4$ for $\widetilde{a}_{0,N}/a_{2,1} < 0$, there is a cusp point on $\eta = 0$, see figures 1(*d*) and 1(*e*).

2.1. *The effect of the Navier–Stokes equations on the topological flow patterns*

The above discussion focuses on the existence of a streamfunction for which only incompressibility is assumed under the mirror symmetry condition. Similar to the analysis by Hartnack (1999*b*) for the flow close to a wall we may now determine which degenerate flow patterns in figure 1(*a–e*) can be seen in steady or unsteady Navier–Stokes equations. This can be performed with the vorticity transport equation:

$$\nu\nabla^4\psi = \frac{\partial\nabla^2\psi}{\partial t} + \frac{\partial\psi}{\partial y}\frac{\partial}{\partial x}(\nabla^2\psi) - \frac{\partial\psi}{\partial x}\frac{\partial}{\partial y}(\nabla^2\psi)$$

where ν is the kinematic viscosity. Inserting the expansion (2) and collecting terms of the same order in x, y gives a series of algebraic equations for the $a_{i,j}$. The equations to order zero, one and two are

$$x^0y^0\colon \nu(24\,a_{4,0} + 8\,a_{2,2} + 24\,a_{0,4}) = a_{0,1}(6\,a_{3,0} + 2\,a_{1,2}) + 2\,\frac{\mathrm{d}}{\mathrm{d}t}a_{2,0} + 2\,\frac{\mathrm{d}}{\mathrm{d}t}a_{0,2} - a_{1,0}(2\,a_{2,1} + 6\,a_{0,3}), \tag{14}$$

$$x^0y^1\colon v(24\,a_{4,1}+24\,a_{2,3}+120\,a_{0,5}) = 6\,\frac{\mathrm{d}}{\mathrm{d}t}a_{0,3}+2\,\frac{\mathrm{d}}{\mathrm{d}t}a_{2,1} + a_{0,1}(6\,a_{3,1}+6\,a_{1,3})+2\,a_{0,2}(6\,a_{3,0}+2\,a_{1,2})-a_{1,0}(4\,a_{2,2}+24\,a_{0,4}) - a_{1,1}(2\,a_{2,1}+6\,a_{0,3}), \tag{15}$$

$$x^1y^0\colon v(24\,a_{1,4}+120\,a_{5,0}+24\,a_{3,2}) = -a_{1,0}(6\,a_{3,1}+6\,a_{1,3}) + a_{1,1}(6\,a_{3,0}+2\,a_{1,2})+6\,\frac{\mathrm{d}}{\mathrm{d}t}a_{3,0}-2\,a_{2,0}(2\,a_{2,1}+6\,a_{0,3})+2\,\frac{\mathrm{d}}{\mathrm{d}t}a_{1,2} + a_{0,1}(4\,a_{2,2}+24\,a_{4,0}), \tag{16}$$

$$x^0y^2\colon v(24a_{4,2}+48a_{2,4}+360a_{0,6}) = a_{0,1}(6\,a_{3,2}+12\,a_{1,4})+2\,a_{0,2}(6\,a_{3,1} + 6\,a_{1,3})+3\,a_{0,3}(6\,a_{3,0}+2\,a_{1,2})+2\,\frac{\mathrm{d}}{\mathrm{d}t}a_{2,2}-a_{1,0}(6\,a_{2,3}+60\,a_{0,5}) - a_{1,1}(4\,a_{2,2}+24\,a_{0,4})-a_{1,2}(2\,a_{2,1}+6\,a_{0,3})+12\,\frac{\mathrm{d}}{\mathrm{d}t}a_{0,4}. \tag{17}$$

$$x^1y^1\colon v(72\,a_{3,3}+120\,a_{1,5}+120\,a_{5,1}) = 6\,\frac{\mathrm{d}}{\mathrm{d}t}a_{1,3}-a_{1,0}(12\,a_{3,2}+24\,a_{1,4}) + 6\,\frac{\mathrm{d}}{\mathrm{d}t}a_{3,1}-2\,a_{2,0}(4\,a_{2,2}+24\,a_{0,4})-2\,a_{2,1}(2\,a_{2,1}+6\,a_{0,3}) + a_{0,1}(24\,a_{4,1}+12\,a_{2,3})+2\,a_{0,2}(4\,a_{2,2}+24\,a_{4,0})+2\,a_{1,2}(6\,a_{3,0}+2\,a_{1,2}), \tag{18}$$

$$x^2y^0\colon v(24\,a_{2,4}+48\,a_{4,2}+360\,a_{6,0}) = -3\,a_{3,0}(2\,a_{2,1}+6\,a_{0,3})+2\,\frac{\mathrm{d}}{\mathrm{d}t}a_{2,2} + a_{0,1}(6\,a_{3,2}+60\,a_{5,0})+a_{2,1}(6\,a_{3,0}+2\,a_{1,2})-2\,a_{2,0}(6\,a_{3,1}+6\,a_{1,3}) + 12\,\frac{\mathrm{d}}{\mathrm{d}t}a_{4,0}-a_{1,0}(6\,a_{2,3}+12\,a_{4,1})+a_{1,1}(4\,a_{2,2}+24\,a_{4,0}). \tag{19}$$

We start by considering the steady case for $N=3$. Under the mirror symmetry condition (3) and all degeneracy and non-degeneracy conditions in Theorem 2.1 ($a_{2,1}\neq 0, a_{0,3}\neq 0$), equations (14)–(19) become zero-except part of equation (18) which is

$$a_{2,1}+3a_{0,3}=0. \tag{20}$$

Equation (20) implies that figure 1(*a*) is possible for a in steady Navier–Stokes equation since the local flow topology was determined by the sign of $a_{0,3}/a_{2,1}$, see equation (10) whereas figure 1(*b*) is not possible. Similar limitations was also obtained by Hartnack (1999*b*) for the degenerate flow patterns in steady flow. For $N\geqslant 4$ equation (20) does not satisfy the non-degeneracy conditions ($a_{0,3}=0$ and $a_{2,1}\neq 0$). Hence the degenerate patterns shown in figure 1(*b–e*) can not occur in the steady flow with the mirror symmetry.

In the unsteady case, the mirror symmetry of the flow is generally broken, except at isolated time instants. For instance, the mirror symmetry of a steady wake is broken when the flow becomes periodic (Brøns *et al.* 2007). The relevant nonlinear equation (18) becomes

$$6\,\frac{\mathrm{d}}{\mathrm{d}t}a_{1,3}(t^*)+6\,\frac{\mathrm{d}}{\mathrm{d}t}a_{3,1}(t^*)-2a_{2,1}(t^*)(a_{2,1}(t^*)+3a_{0,3}(t^*))=0 \tag{21}$$

at some time instant t^*. The time derivatives in (21) are identically zero when the flow is symmetric for all times, but they will in general be non-zero, even at a specific time instant where symmetry occurs such that $a_{3,1}=a_{1,3}=0$, which is the relevant case for all practical purposes, and here no general conclusions about topology can be drawn.

For Stokes flow (as $\nu \to \infty$ in the vorticity transport equation), since the right-hand side of equations (14)–(19) becomes zero, the left-hand side gives us no information about $a_{2,1}$ and $a_{0,N}$. So the transformed parameter $\widetilde{a}_{0,N}$ can be chosen as free parameter. Thus, the non-degeneracy conditions in Theorem 2.1 must hold and the degenerate flow patterns in figure 1(*b–e*) are possible in Stokes flow.

2.2. *Unfolding of non-simple degenerate critical points*

The degenerate flow patterns obtained in the previous section will appear only when the coefficients $a_{0,1}$, $a_{2,0}$ and $a_{0,2}$ are zero. In this section, to determine all possible bifurcations close to non-simple degenerate critical points, we consider a small perturbation of these coefficients as the bifurcation value in the streamfunction. The method for finding the normal form of unfolding of non-simple degenerate critical points proceeds exactly as in previous studies (Brøns & Hartnack 1999; Gürcan & Deliceoglu 2005). We omit computations and only give the result by the following theorem.

THEOREM 2.2. *Let $a_{0,1}$, $a_{2,0}$, $a_{0,2}$ and $\widetilde{a}_{0,3}, \ldots, \widetilde{a}_{0,N-1}$ be small parameters. Assuming the non-degeneracy conditions $a_{2,1} \neq 0$ and $\widetilde{a}_{0,N} \neq 0$ are satisfied, then a normal form of order N for the stream function (4) is*

$$\psi_N(x, y) = y(\sigma x^2 + f(y)), \quad f(y) = \sum_{i=0}^{N-1} b_i y^i, \quad b_{N-1} = 1, \tag{22}$$

where

$$\sigma = \begin{cases} +1 & \text{for } \widetilde{a}_{0,N-1}/a_{2,1} > 0, \\ -1 & \text{for } \widetilde{a}_{0,N-1}/a_{2,1} < 0. \end{cases} \tag{23}$$

and $b_i, i = 0, \ldots, N-2$ are transformed small parameters.

Using the normal form (22), the corresponding dynamical system,

$$\begin{aligned} \dot{x} &= \sigma x^2 + f(y) + y f'(y), \\ \dot{y} &= -2\sigma x y, \end{aligned} \tag{24}$$

with the Jacobian

$$\boldsymbol{J} = \begin{pmatrix} 2\sigma x & 2f'(y) + y f''(y) \\ -2\sigma y & -2\sigma x \end{pmatrix} \tag{25}$$

can be analysed. Evaluating $|\boldsymbol{J}|$ from (25) we obtain

$$|\boldsymbol{J}| = -4x^2 + 2\sigma y(2f'(y) + y f''(y)). \tag{26}$$

The normal form for system (22) contains the x-axis as a streamline for $\psi = 0$. A simple calculation of $|\boldsymbol{J}|$ shows that critical points on the x-axis corresponding to (24) for $y = 0$ are saddle points given by

$$(x, y) = (\pm\sqrt{-\sigma b_0}, 0)$$

and there is a bifurcation for $b_0 = 0$.

Off the x-axis corresponding to (24) for $x = 0$ critical points satisfy $x = 0$, $f(y) + y f'(y) = 0$. Local bifurcation of critical points off the x-axis occurs for $2f'(y) + y f''(y) = 0$ and the critical point is a centre if σy and $(2f'(y) + y f''(y))$ have the same sign. The vorticity is

$$\omega = \nabla^2 \psi_N = 2\sigma y + 2f'(y) + y f''(y). \tag{27}$$

Since the vorticity depends upon the sign of σy, the vortices or eddy patterns have opposite rotations with respect to the x-axis.

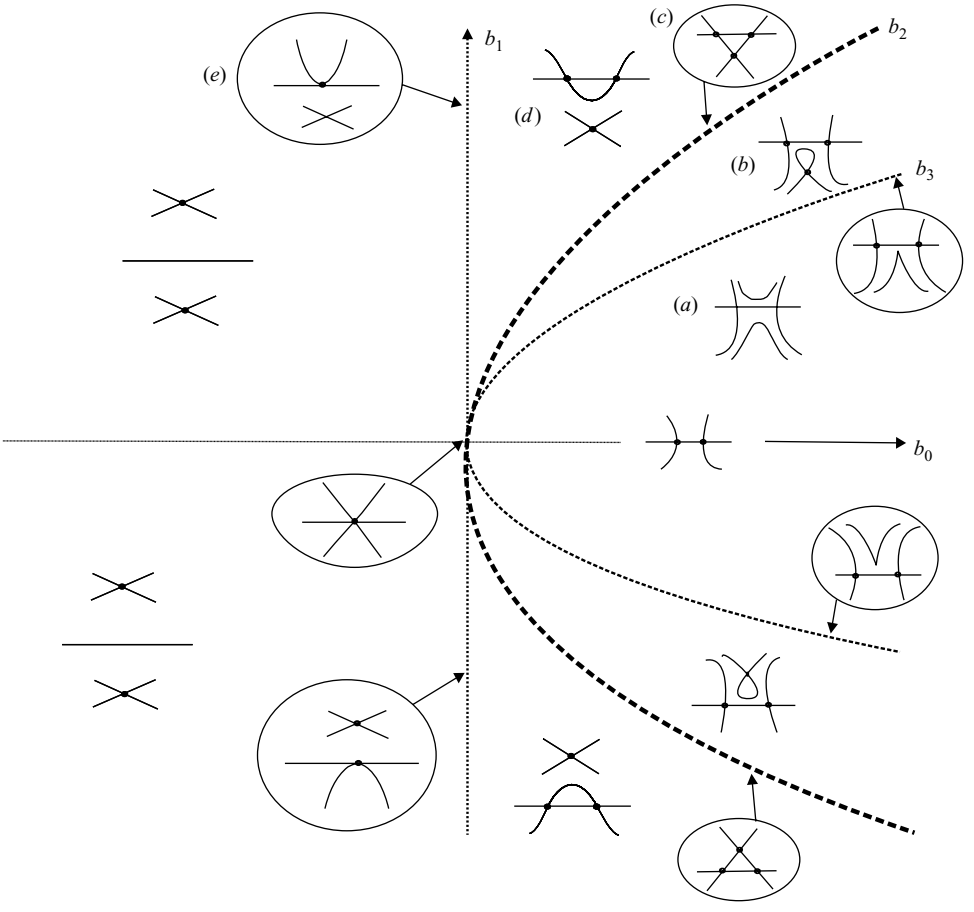

FIGURE 2. Illustration of a bifurcation diagram of the third-order normal form for $\sigma = -1$ with flow patterns away from the wall. A similar diagram was also found by Bakker (1991) and Hartnack (1999*b*) for flows close to a wall.

2.2.1. *Normal form of order 3*

The third order-normal form of the streamfunction is

$$\psi_3 = y(\sigma x^2 + b_0 + b_1 y + y^2). \tag{28}$$

The reader will note that the normal form (28) is almost the same – except the factor y – as the normal form of Bakker (1991) and Hartnack (1999*b*), who have the factor y^2. This difference stems from the boundary conditions taken as the fixed wall in their work. Although, in the present study, the non-simple degenerate critical points are away from boundaries, the flow patterns and their bifurcations are exactly the same as in Bakker (1991) and Hartnack (1999*b*), but with the fixed wall replaced by a streamline. Also, it is interesting that the normal form (22) has a factor y. This means that the x-axis is always a streamline. Hence, the symmetry implies that the analysis by Brøns (1994) of the flow close to a given streamline is relevant here, and it is then no surprise that the bifurcation diagrams are the same as found in Brøns (1994). The relevant computations are omitted and bifurcation diagrams are illustrated in figure 2 for $\sigma = -1$ and in figure 3 for $\sigma = 1$.

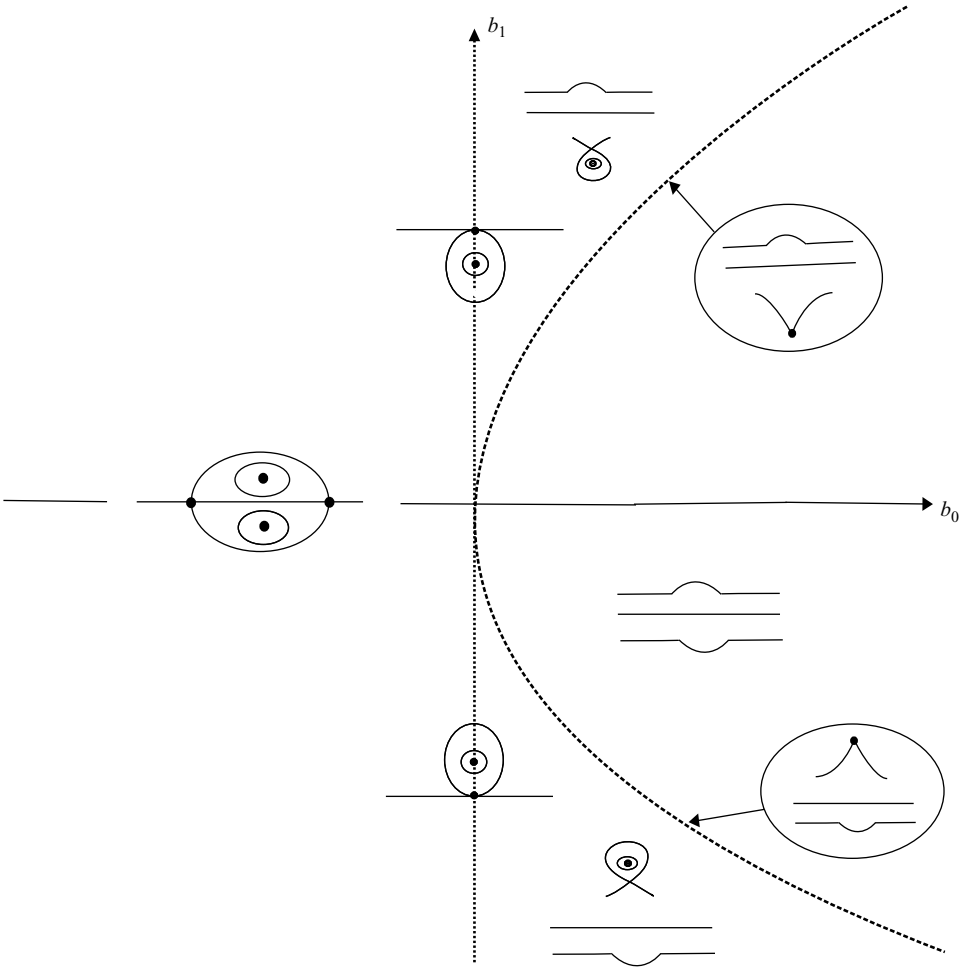

FIGURE 3. Illustration of a bifurcation diagram of the third-order normal form for $\sigma = 1$ with flow patterns away from the wall. Hartnack (1999*b*) presented a similar diagram corresponding to flow close to a wall.

Figure 2 shows a triangle-bifurcation that consists of three saddle points each of which lies at the corner of a triangle connected by a single heteroclinic connection. This pattern is numerically observed in the double-lid-driven cavity flow problem.

2.2.2. *Cavity flow*

Stokes flow in a double-lid-driven rectangular cavity with two solid walls and two moving lids is governed by the biharmonic equation for the streamfunction ψ

$$\nabla^4 \psi = 0. \tag{29}$$

The boundary conditions (no-slip and impermeability) and non-dimensionalization can be found in detail, for example, in Gürcan *et al.* (2003). In this problem, there are two physical parameters: the cavity aspect ratio, A (height to width) and the speed ratio, S (the ratio of the upper to the lower lid velocities). Following Gürcan (1997) and Joseph Sturges (1978) the general solution for the streamfunction for any value

of S and A can be written as

$$\psi = \sum_{n=-\infty}^{\infty} \{A_n e^{s_n(y-A)} + B_n e^{-s_n(y+A)}\} \frac{\phi_1^n(x, s_n)}{s_n^2}, \tag{30}$$

where the s_n are complex eigenvalues and the functions ϕ_1^n are even Papkovich–Faddle eigenfunctions, satisfying the no-slip boundary conditions on the sidewalls. For the Stokes flow solution (30) the symmetry condition (3) holds, as the functions ϕ_1^n are even functions of x. Furthermore, the mirror symmetry condition of the analytic solution (30) is not relevant for Navier–Stokes flow in which there will be asymmetric solutions even for small Re.

A_n and B_n are complex coefficients determined using a truncation technique employing Smith's (1952) biorthogonality relation which yields $2N$ equations for the $2N$ unknowns. It is found computationally that for all aspect ratios and speed ratios investigated, $A \in [0.05, 7]$ and $S \in [-1, 1]$, as n increases $A_n = O(1/n^2)$, $B_n = O(1/n^2)$ and hence this procedure converges because of the strong influence of the exponential factor in the solution (30). When the coefficients have been determined, the streamfunction at any interior point in the liquid is obtained by simply summing a finite number of terms in the series (30) while ensuring that the magnitude of the truncation error is acceptably small, see Gürcan *et al.* (2003). Figure 4 in the present paper was produced using a truncation number of $N = 200$.

2.2.3. *Special Streamline Patterns*

A detailed exploration of flow structures and eddy genesis in the double-lid-driven cavity has been conducted by Gürcan, Wilson & Savage (2006), with particular attention given to explaining the repetition of bifurcation patterns in terms of local symmetries in the cavity. Their work and that of Gürcan & Deliceoğlu (2006) showed a global bifurcation with a single heteroclinic connection between three saddle points, each lying at the corner of a triangle. These flow bifurcations are good examples for an application of the above theoretical work. The sequence of flow patterns reproduced in figure 4 shows more clearly the construction and breaking of the triangle-bifurcation, see figure 4(*b–d*).

By tracking these bifurcations we produce a control-space diagram via the following scheme: We first determine the position of stagnation points (say (x_s, y_s)) in the cavity which are solutions of

$$u((x, y), S, A) = v((x, y), S, A) = 0,$$

by using a bisection method with a tolerance of 10^{-10} for each A and S where A and S are varied with very small steps in $4.5 < A < 4.75$ and $-0.0035 < S < -0.002$. Then to determine the nature of a particular stagnation point (saddle or centre) the streamfunction (30) is expanded as a Taylor series about that point, see Gaskell *et al*. (1998). To obtain the triangle-bifurcation (b_2 in figure 5) we examine the values of the series (30) at the saddle points. If (30) gives the same values at those points, then b_2 occurs. The saddle node (cusp) bifurcation curve, b_3, is obtained when a saddle and centre are born simultaneously on $x = 0$ in the cavity at which u changes sign. Finally, as the saddle points on either side of $x = 0$ (see figure 4*d*) approach the centre on $x = 0$ and meet, there is a bifurcation (b_1 in figure 5) producing a saddle on $x = 0$ (figure 4*e*).

Figure 5 shows a control-space diagram with bifurcation curves which exhibit local symmetry about the line $S_c = -0.0028$. For $S < S_c$, the flow development sequence in the middle eddy follows a similar pattern to that in the upper eddy in the

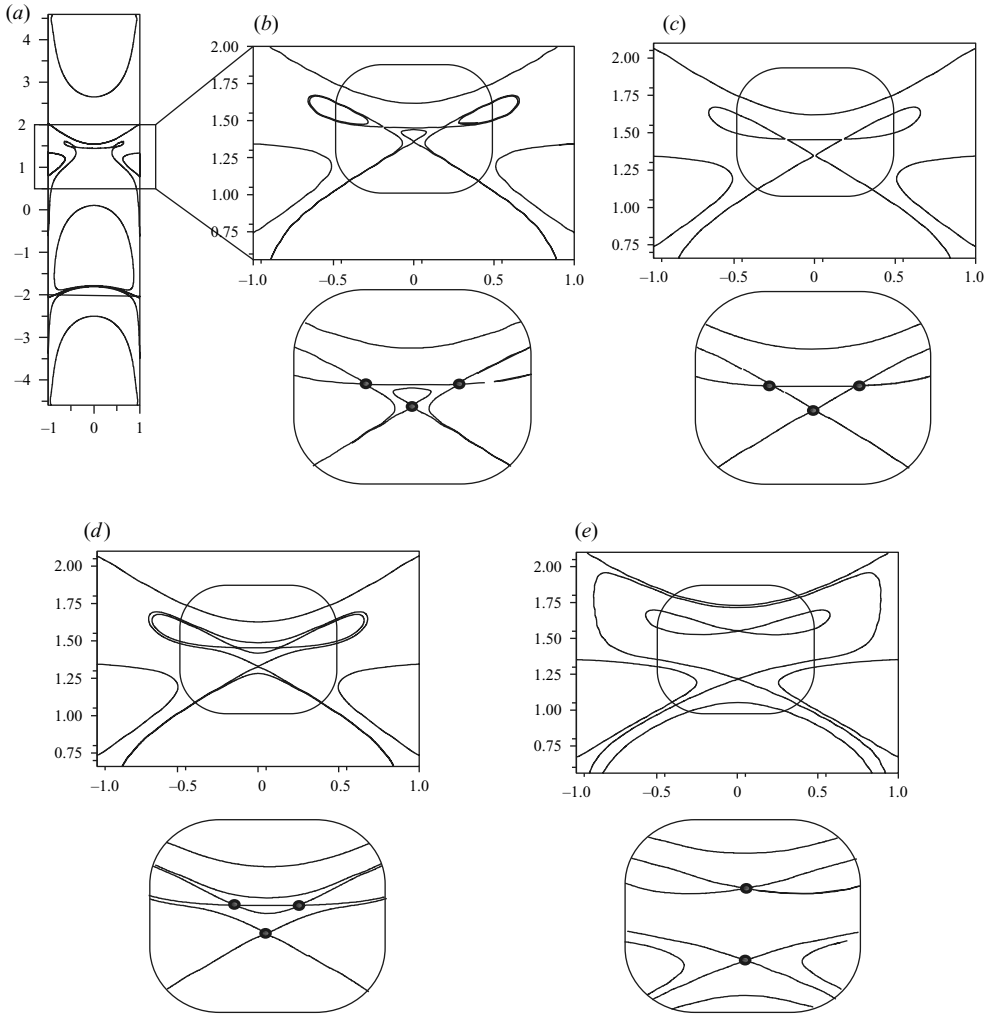

FIGURE 4. Flow structure development in the upper section of the double-lid-driven cavity as A increases from 4.6 for $S = -0.0031$; in (a) a full cavity is shown with $A = 4.6$, and in (b–e) enlarged views of two parts of cavity are shown. The first is an enlarged view of the rectangular part in (a) and the second is an enlarged view of the oval part in (b–e) for (b) $A = 4.624$, (c) $A = 4.6321$, (d) $A = 4.645$, (e) $A = 4.678$.

cavity for $S > S_c$, see streamlines in the cavities at the bottom of figure 5. When $S = S_c$ the upper and middle eddies become symmetric about their shared separating streamline (for example see the top cavity in figure 5) because the ratio of the upper lid velocity (S_c) and the separating streamline velocity near the lower eddy (say $S_l = u(x_l, y_l)$ where (x_l, y_l) is the position of the separating streamline II) is equal to $S_c/S_l \cong -1$. The pattern in the top cavity for $(A, S) = (4.625, S_c)$ represents the pattern at an intersection point of the bifurcation curves in figure 5 that shows the double symmetry in the upper part of the cavity.

In conclusion, we found that the flow bifurcations (b_1, b_2, b_3) in figure 5 are exactly the same as in those of figure 2. In each figure, corresponding flow patterns and bifurcation curves are labelled with the same letters. The pattern at the origin $(b_0, b_1) = (0, 0)$ in figure 2 is exactly the same as the pattern about the point P in the

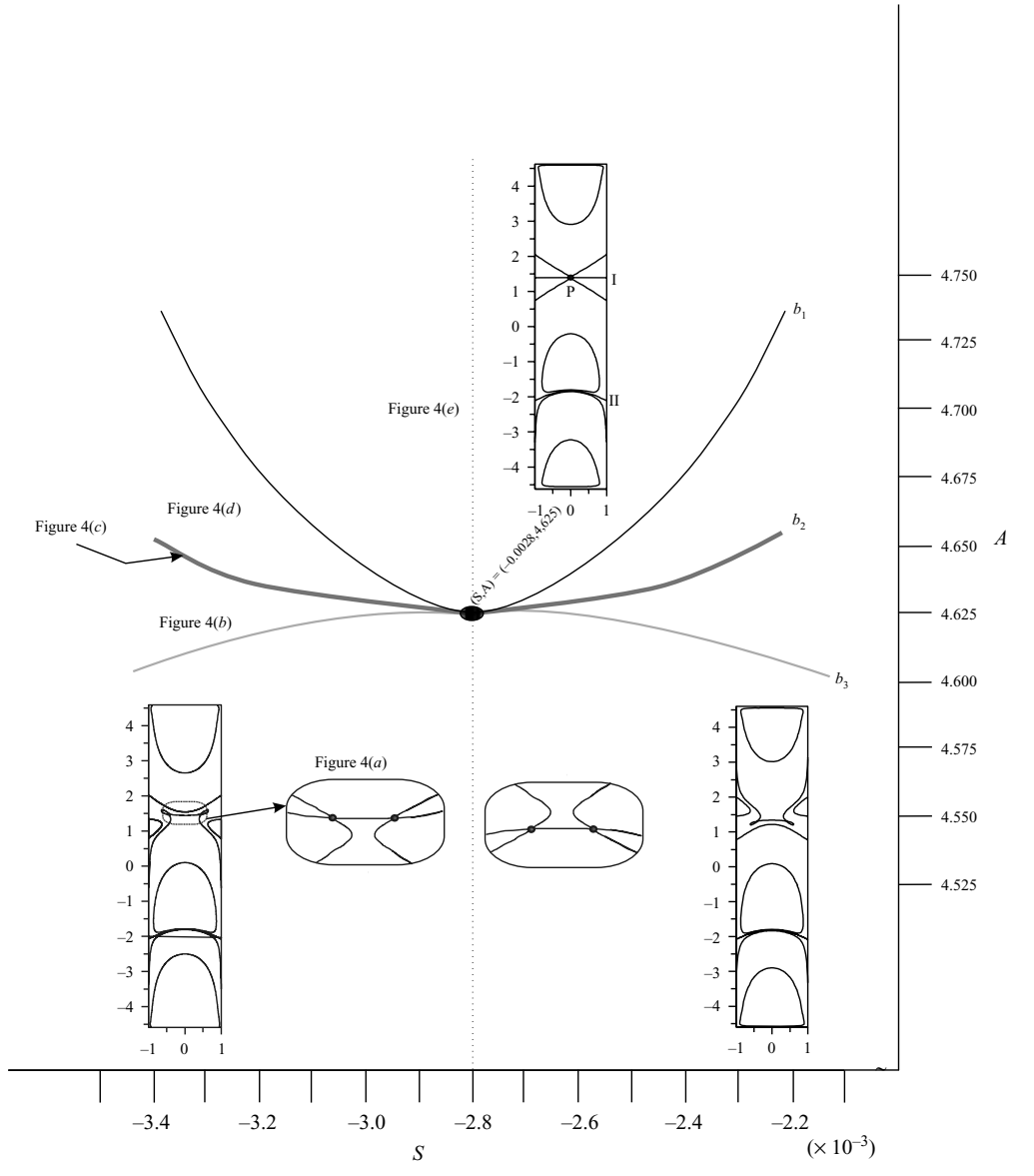

FIGURE 5. Control-space diagram for the double-lid-driven cavity when $4.5 < A < 4.75$ and $-0.0035 < S < -0.002$. The flow patterns associated with each region are referred to figure 4 and three typical flow patterns are illustrated.

top cavity in figure 5. The line $S_c = -0.0028$ in figure 5 corresponds exactly to the line $b_1 = 0$ in figure 2. When the S_c is crossed there is no change in flow topology in the enlarged oval part of the cavity and double symmetry can only appear.

2.2.4. *Normal form of order 4*

The fourth-order normal form of the streamfunction is given by

$$\psi_4 = y(x^2 + b_0 + b_1 y + b_2 y^2 + y^3). \tag{31}$$

The corresponding dynamical system with codimension two is

$$\left.\begin{aligned}\dot{x} &= x^2 + b_0 + 2b_1 y + 3b_2 y^2 + 4y^3,\\ \dot{y} &= -2xy.\end{aligned}\right\} \tag{32}$$

The locations of the critical points on the x-axis ($y=0$) are $x = \pm\sqrt{-b_0}$ and there is a bifurcation line for $b_0 = 0$.

Off the x-axis ($x=0$), local bifurcations occur when

$$\left.\begin{aligned}b_0 + 2b_1 y + 3b_2 y^2 + 4y^3 &= 0,\\ b_1 + 3b_2 y + 6y^2 &= 0.\end{aligned}\right\} \tag{33}$$

Combining these, one obtains

$$96b_1^3 - 27b_1^2 b_2^2 - 324b_1 b_2 b_0 + 324b_0^2 + 81b_0 b_2^3 = 0. \tag{34}$$

The conditions for global bifurcation are

$$\left.\begin{aligned}\frac{\partial \psi}{\partial y}(0, y) &= b_0 + 2b_1 y + 3b_2 y^2 + 4y^3 = 0,\\ \psi(0, y) &= b_0 + b_1 y + b_2 y^2 + y^3 = 0,\end{aligned}\right\} \tag{35}$$

and combining these gives

$$27b_0^2 - 18b_0 b_1 b_2 + 4b_0 b_2^3 - b_1^2 b_2^2 + 4b_1^3 = 0. \tag{36}$$

To analyse flow patterns in three parameters is rather academic. Therefore, we analyse first the case $b_1 = 0$ and then consider $b_1 > 0$.

To reduce parameter number we can use the parameterisation

$$b_0 = k(b_1/3)^{3/2} \quad \text{and} \quad b_2 = l(b_1/3)^{1/2}. \tag{37}$$

We find that bifurcation sets for $b_1 \neq 0$ become:

$$k = 0 \quad \text{and} \quad 32 - 3l^2 - 12kl + 4k^2 + kl^3 = 0, \tag{38}$$

and global bifurcations occur for

$$27k^2 - 54kl + 4kl^3 - 9l^2 + 108 = 0. \tag{39}$$

The complete bifurcation diagram is shown in figures 6 and 7. The existence of the above structure allows us to recognize different flow patterns in Stokes flow, but the degenerate flow patterns figure 1(*d*) 1(*e*) cannot be realized physically since they require some parameters to be zero.

3. Conclusion

The results of the present study show that the normal form method which was first applied by Brøns & Hartnack (1999) for the simple degeneracy works also for the non-simple degeneracy under the mirror symmetry condition. The normal form transformation gives us a framework for investigating the process of streamline pattern development and their bifurcations up to codimension three. We extend the classification of possible local streamline topologies in two-dimensional incompressible flow by using the normal form transformation. To our knowledge the degenerate flow pattern 'the cusp on the axis' (fourth-order non-simple degeneracy) and its bifurcation patterns has not been previously observed theoretically in Stokes flow.

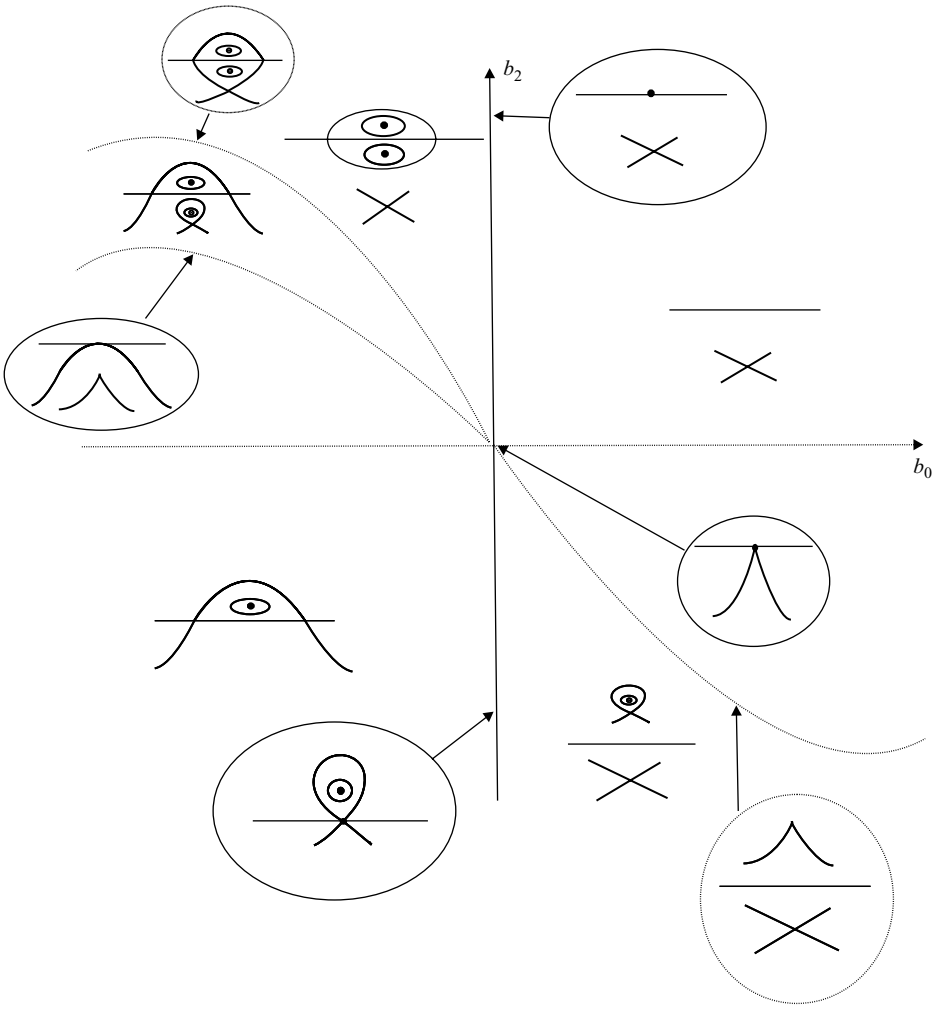

FIGURE 6. Bifurcation diagram of the fourth-order normal form with $b_1 = 0$.

For codimension two, the normal form and corresponding bifurcation diagrams which were found near the wall by Bakker (1991) and Hartnack (1999*b*) are also observed away from the wall. The theoretical results are applied to analyse numerical solutions of Stokes flow in a cavity flow as a configuration physically accommodating patterns corresponding to the normal form of order 3 and we review some of the results of Gürcan & Deliceoğlu (2006).

The Navier–Stokes equations in which there will be asymmetric solutions even for small Re restrict the local flow topology under the symmetry condition (3). It was shown that for codimension three all flow patterns and their bifurcations away from the wall occur in Stokes flows, and in (unsteady) 'Navier–Stokes' flows no general conclusion about topology can be drawn. In contrast to the simple degeneracies, we have seen that the interaction of all vortices or eddy patterns have opposite rotations with respect to the x-axis in non-simple degeneracies. These feature provides some interesting and important patterns that cannot seen near the simple degeneracies. For example, the particular 'triangle' heteroclinic connection and a homoclinic connection

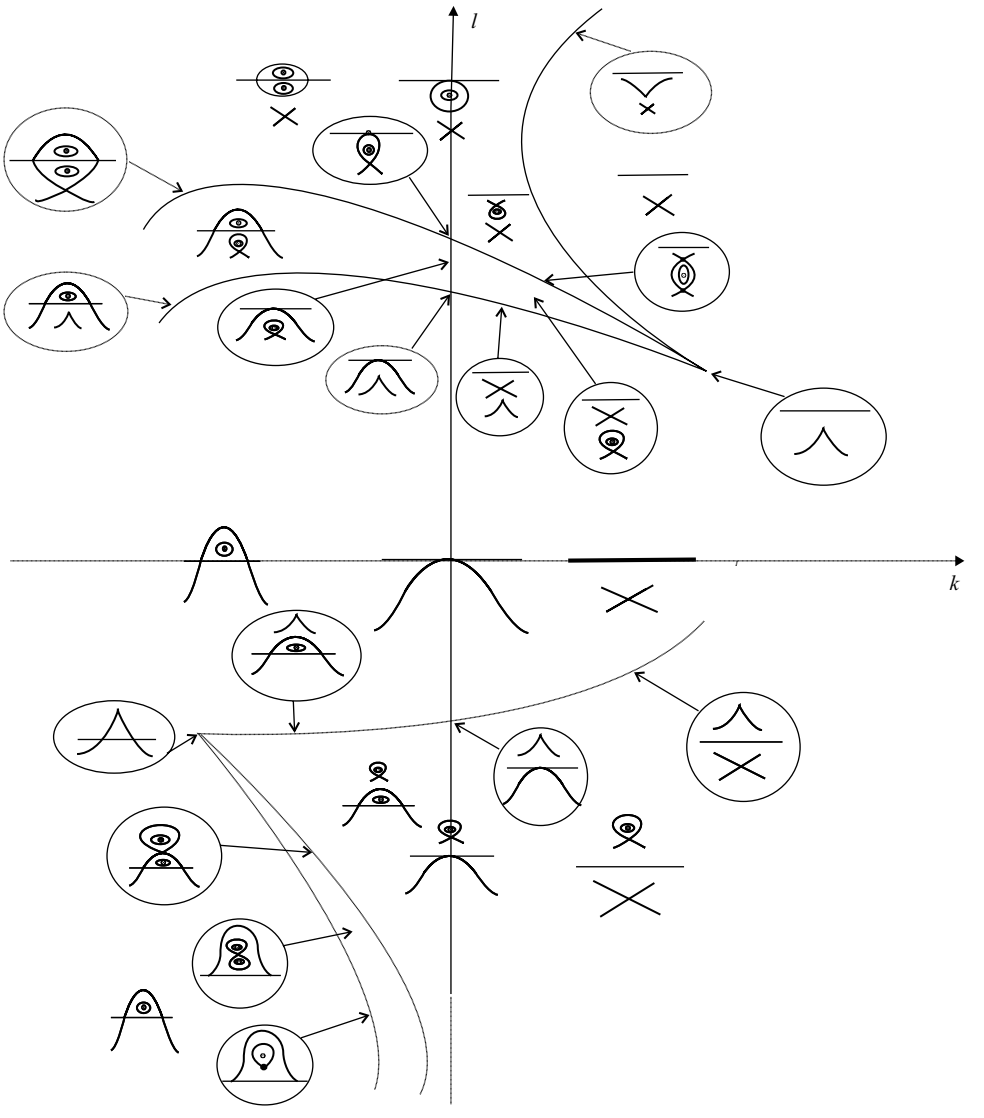

FIGURE 7. Bifurcation diagram of the fourth-order normal form with $b_1 > 0$.

on the x-axis are just as an one of the unfoldings of the third- and fourth-order non-simple degeneracy.

The authors are grateful to all reviewers for their helpful suggestions.

REFERENCES

BRØNS, M. 1994 Topological fluid dynamics of interfacial flows. *Phys. Fluids* **6**, 2730–2737.

BRØNS, M. 2007 Streamline topology-Patterns in fluid flows and their bifurcations. *Adv. Appl. Mech.* **41**, 1–43.

BRØNS, M. & BISGAARD, A. V. 2006 Bifurcation of vortex breakdown patterns in a circular cylinder with two rotating covers. *J. Fluid Mech.* **568**, 329–349.

Brøns, M. & Hartnack, J. N. 1999 Streamline topologies near simple degenerate critical points in two-dimensional flow away from boundaries. *Phys. Fluids* **11**, 314–324.

Brøns, M., Jakobsen, B., Niss, K., Bisgaard, A. V. & Voigt, L. K. 2007 Streamline topology in the near-wake of a circular cylinder at moderate Reynolds numbers. *J. Fluid Mech.* **584**, 23–43.

Brøns, M., Voigt, L. K. & Sørensen J. N. 1999 Streamline topology of steady axisymmetric vortex breakdown in a cylinder with co- and counter-rotating end-covers. *J. Fluid Mech.* **401**, 275–292.

Brøns, M., Voigt, L. K. & Sørensen J. N. 2001 Topology of vortex breakdown bubbles in a cylinder with a rotating bottom and a free surface. *J. Fluid Mech.* **428**, 133–148.

Bakker, P. G. 1991 *Bifurcation in Flow Patterns.* D. Klüwer.

Bisgaard, A. V., Brøns, M. & Sørensen, J. N. 2006 Vortex breakdown generated by off-axis bifurcation in circular cylinder with rotating covers. *Acta Mechanica* **187**, 75–83.

Chien, W. L., Rising, H. & Ottino, J. M. 1986 Laminar mixing and chaotic mixing in several cavity flows. *J. Fluid Mech.* **170**, 355–377.

Dallmann, U. 1983 Topological structures of three-dimensional flow separations. IB 221–82 A 07. DFVLR.

Dallmann, U. & Gebing, H. 1994 Flow attachment at flow separation lines. *Acta Mechanica* **4**, 47.

Gaskell, P. H., Gürcan, F., Savage, M. D. & Thompson, H. M. 1998 Stokes flow in a double-lid-driven cavity with free surface side-walls. *Proc. Inst. Mech. Engrs* C **212**, 387–403.

Gürcan, F. 1997 Flow bifurcations in rectangular, lid-driven, cavity flows. PhD thesis, University of Leeds.

Gürcan, F. 2003 Streamline topologies in Stokes flow within lid-driven cavities. *Theor. Comput. Fluid Dyn.* **17**, 19–30.

Gürcan, F. & Deliceoğlu, A. 2005 Streamline topologies near non-simple degenerate points in two-dimensinonal flows with double symmetry away from boundaries and an application. *Phys. Fluids* **17**, 093106.

Gürcan, F., Gaskell, P. H., Savage, M. D. & Wilson, M. C. T. 2003 Eddy genesis and transformation of Stokes flow in a double-lid driven cavity. *Proc. Inst. Mech. Engrs* C **217**, 353–364.

Gürcan, F. & Deliceoğlu, A. 2006 Saddle connections near degenerate critical points in Stokes flow within cavities. *Appl. Math. Comput.* **172**, 1133–1144.

Gürcan, F., Wilson, M. C. T. & Savage, M. D. 2006 Eddy genesis and transformation of Stokes flow in a double-lid driven cavity Part 2: deep cavity. *Proc. Inst. Mech. Engrs.* C **220**, 1765–1774.

Hartnack, J. N. 1999 Structural changes in incompressible flow patterns. PhD thesis, Department of Mathematics, Technical University of Denmark.

Hartnack, J. N. 1999 Streamlines topologies near a fixed wall using normal forms. *Acta Mechanica* **136**, 55–75.

Joseph, D. D. & Sturges, L. 1978 The convergence of biorthogonal series for biharmonic and Stokes flow edge problems: Part II. *SIAM. J. Appl. Maths* **34**, 7–27.

Legendre, R. 1956 Séparation de I'écoulement laminaire tridimensionel. *Rech. Aerosp.* **54**, 3–8.

Meleshko, V. V. 1996 Steady Stokes flow in a rectangular cavity. *Proc. R. Soc. Lond.* A **452**, 1999–2022.

Milne-Thomson, L. M. 1957 A general solution of the equations of hydrodynamics. *J. Fluid Mech.* **2**, 88.

Milne-Thomson, L. M. 1968 *Theoretical Hydrodynamics.* Dover.

Shankar, P. N. & Deshpande, M. D. 2000 Fluid mechanics in the driven cavity. *Annu. Rev. Fluid Mech.* **32**, 93–136.

Smith, R. C. T. 1952 The bending of a semi-infinite strip. *Austral. J. Sci. Res.* **5**, 227–237.

Tobak, M. & Peake, D. J. 1982 Topology of three-dimensional separated flows. *Annu. Rev. Fluid Mech.* **14**, 61–85.

Tophøj, L., Møller, S. & Brøns, M. 2006 Streamline patterns and their bifurcations near a wall with Navier slip boundary conditions. *Phys. Fluids* **18**, 083102.